

# TRACKING DISPLACEMENTS OF INTRACELLULAR ORGANELLES IN RESPONSE TO NANOMECHANICAL FORCES

Yaron R. Silberberg<sup>1</sup>, Andrew E. Pelling<sup>1</sup>, Gleb E. Yakubov<sup>2</sup>, William R. Crum<sup>3</sup>, David J. Hawkes<sup>3</sup> and Mike A. Horton<sup>1</sup>

<sup>1</sup>The London Centre for Nanotechnology and Centre for NanoMedicine, University College London, 17-19 Gordon Street, London, WC1H 0AH, United Kingdom.

<sup>2</sup>Unilever Corporate Research, Colworth Park, Sharnbrook, Bedfordshire, MK44 1LQ, United Kingdom.

<sup>3</sup>Centre for Medical Image Computing (CMIC), Malet Place Engineering Building University College London, Gower Street, London WC1E 6BT, United Kingdom.

## ABSTRACT

The living cell is under constant influence of mechanical forces from its environment. These forces affect many aspects of the cell's behaviour, including morphology, growth, cell differentiation, protein synthesis and cell death. In this study we show how mechanical stress perturbs the intracellular structures of the cell and induces mechanical responses. In order to correlate mechanical perturbations to cellular responses, we used a combined fluorescence-atomic force microscope (AFM) to produce nanomechanical perturbations while simultaneously tracking the real-time motion of fluorescently labelled mitochondria in live cells. Feature point tracking was then used to analyze and quantify the structural displacements. Following indentation from the AFM tip, the average mitochondrial displacement showed an increase of ~40% in comparison to the natural movement. These results show how mitochondrial structures that are far away from the point of force (up to ~40  $\mu\text{m}$ ) are instantaneously affected by extracellular perturbations.

**Index Terms**— Atomic Force Microscopy; fluorescence microscopy; mitochondria; nanomechanics; mechanotransduction; particle tracking

## 1. INTRODUCTION

The Atomic Force Microscope (AFM) [1] has become an invaluable tool for investigating biological systems. The ability to study living cells in fluid under physiological conditions has facilitated both nano-scale imaging [2] and the measurement of various mechanical and material properties of living cells, such as viscoelasticity [3, 4] and mechanical dynamics [5, 6]. Recent technical developments have integrated traditional microscopy methods, such as fluorescence and laser scanning confocal microscopies, into AFM systems [7]. This has enabled the simultaneous measurement of material properties of living cells and their biological responses and signalling pathways to be made.

In this work we investigated the effect of nano-scale mechanical forces on the living cell by inspecting the displacement of intracellular organelles in response to extracellular forces. In this case, mitochondrial displacements were tracked following perturbations produced by the AFM tip. We have examined and quantified the natural movement and force-induced displacement of mitochondria using a feature point tracking algorithm [8] that is integrated in the ImageJ plugin 'ParticleTracker'. This algorithm enables an efficient, automated, two-dimensional detection and tracking analysis of particles trajectories. The method is well suited to digital video time-lapse fluorescence imaging which typically generates low-intensity data. Feature point tracking detects particle positions in a digital video sequence and generates particle trajectories over time. One of its main advantages is that it does not make any assumptions regarding the smoothness of the trajectories. Thus, it is extremely useful for many biological applications where the type of motion is not explicitly known in advance. Furthermore, by not assuming a motion model, the algorithm integrity is not biased when several modes of motion are incorporated by a single trajectory. Therefore, this method is ideal for use when tracking both natural and induced motion (post-perturbation) of an organelle in the same time-lapse sequence, such as in this case.

Feature point tracking has been successfully used for different biological applications, including tracking viruses and virus-like particle trajectories on or within living cells [8-10]; investigating individual membrane microdomains in relationship to the cytoskeleton [11]; analyzing cargo movement of microtubules [12]; trafficking of particles during phagocytosis [13]; and cell migration [14].

In this study we focus on the motion of fluorescently-tagged mitochondria in live cells. The nature of the tracking involved made the feature point tracking algorithm a good candidate to use, for two main reasons: first, the particle-like geometry of the mitochondrial structures facilitates easy tracking of their centroid; second, the robustness and flexibility of the algorithm allows different modes of motion to be accepted for single trajectories, as discussed earlier. In

addition, the MitoTracker Red stain [15] used is highly specific for live mitochondria, and only fluoresces once in contact with the mitochondrial membrane, giving a high signal-to-noise ratio.

Using the method of feature point tracking (Materials and Methods) we tracked the displacement of individual mitochondrial structures over time. We then used this information to calculate the absolute displacements of several mitochondrial structures (between 10-30 structures per cell), both before and after the application of extracellular stress using the AFM tip. This allowed us to examine whether, and to what extent, local nanomechanical perturbations affect the force-induced displacement of mitochondria.

## 2. MATERIALS AND METHODS

**Cell culture.** NIH-3T3 Fibroblasts were cultured in DMEM GlutaMAX I media (Invitrogen) supplemented with 10% fetal bovine serum (Sigma) and 100 IU/ml penicillin and 100  $\mu$ g/ml streptomycin (Sigma), at 37 °C in 5% CO<sub>2</sub> atmosphere. Cells were plated into 60mm plastic culture dishes (Orange Scientific) one day prior to the experiment (3ml of media at cell concentration of  $\sim$ 104 cells/ml).

**Fluorescence and Atomic Force Microscopy.** Cells were stained and then placed in a combined AFM-fluorescence microscope (Olympus IX71 inverted optical microscope and JPK NanoWizard® AFM). The temperature controlled stage was maintained at 37°C for the duration of the experiment. MSCT-AUWH tips (Veeco) were calibrated and the spring constant was experimentally measured to be  $0.05 \pm 0.01$  N/m [16]. Single interphase cells were chosen optically and the tip was positioned above the nucleus [17]. At this point, fluorescence imaging was initiated and images were acquired at 1 Hz using a Hamamatsu ORCA-ER camera.

**Feature point tracking algorithm.** The feature point tracking algorithm [8] employs two main steps: the detection of feature points in every frame and the linking of these points into trajectories. The detection step itself is divided into several stages that include image restoration and noise reduction, estimation and refinement of point locations, and non-particle discrimination. User-defined parameters that are required here include the size (in pixels), which should be bigger than a single point radius but smaller than the distance between two separate points. In addition, a percentile parameter is needed that is used to determine the sensitivity of the algorithm to background noise, when deciding the local maxima of featured points. When estimating the feature point locations, the algorithm looks for local intensity maxima. This process is performed on a per-frame basis to eliminate the effect of a reduction in the overall intensity in time, such as in the case of photo-bleaching. When refining the location of the detected points, the assumption made is that a calculated local maximum is near the actual geometric centre of the object. In order to

reduce noise-induced positioning errors, an offset is calculated that is the distance to the brightness-weighted centroid of the object.

The linking algorithm identifies points that correspond to the same physical particle in subsequent frames, linking the positions into trajectories. This is achieved by finding the optimal associations between point locations on different matrices, considering several frames, so as to account for particle occlusion. However, due to the dynamic nature of mitochondria in living cells and the short distances between separate mitochondrial structures, we have manually verified each of the calculated trajectories in order to make sure that there is no false linking of different structures between frames. By verifying both the automated detection and the linking process, we can minimize the chances of false detections and linking due to low signal-to-noise ratio.

## 3. RESULTS

**Local forces produce structural perturbations.** Mitochondria form dense three-dimensional networks around the nucleus and become flattened and more sparsely distributed at the edges of the cell (Figure 1, A). Here, we have examined how locally applied forces above the nucleus are physically transmitted over long distances to the cell edge (Figure 1, B). We limited our analysis to the cell edge (Figure 1, C, D) where it is very flat, as little as 200nm thick, and mitochondria are assumed to move in two dimensions. Individual mitochondria can be resolved much more clearly in these regions, allowing a more accurate image registration and tracking analysis to be performed.

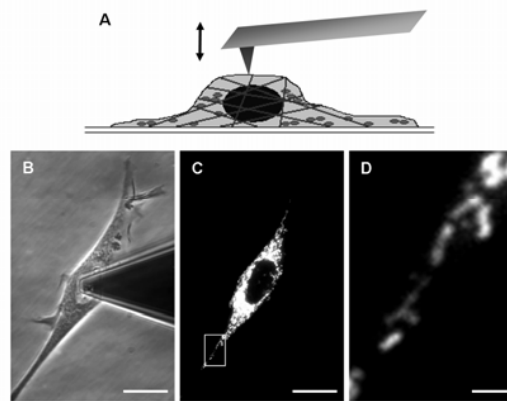


**Figure 1.** (A) Schematic illustration of an AFM tip above a living cell (mitochondria are indicated as spherical particles). (B) Phase-contrast image of an AFM tip in contact with a living cell. (C) Fluorescent image of mitochondria. The cell was stained using MitoTracker (Invitrogen) mitochondria live-cell marker. (D) Magnified section showing distinguishable mitochondrial structures. Scale bars: B-C: 20  $\mu$ m; D: 2  $\mu$ m.

Mitochondria are dynamic structures, which display basal movements driven by the cytoskeleton. In order to distinguish natural displacements from those caused by the

AFM tip, we designed the following experiment which includes a built-in control for each cell. Images were captured at 1 frame/sec, followed by perturbation with the AFM tip with a force of 10nN (Figure 1, B). To quantify mitochondrial displacements, tracking analysis was conducted on three sequential frames with the cell at rest in the first two frames and perturbed using the AFM tip between the second and third frame. Pre-perturbation mitochondrial motion (i.e. natural motion) was calculated between frames 1 and 2, and post-perturbation motion between frames 2 and 3. The mean displacements of each mitochondrial structure in the selected regions were then calculated for both pre- and post-perturbation trajectories. Typically, 2 regions were selected for each cell and  $n = 10$ -30 mitochondria were tracked per cell.

For each cell measured ( $n=21$ ), displacements were calculated for the average basal displacements in addition to the average perturbed displacements of individual mitochondrial structures ( $n=323$ , for all cells). Figure 2 shows a fluorescent image of the cell under perturbation with the AFM tip. The point of perturbation can be clearly seen as an 'x' shape in the centre of the cell (Figure 2A). A region of interest was chosen (Figure 2A, white square), and trajectories of displacement were generated (Figure 2B, lines represent trajectories of individual mitochondria). Later, the magnitude of displacement was calculated, and compared to that of the natural mitochondrial movement.

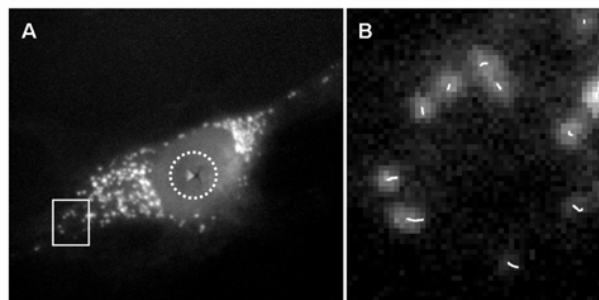


**Figure 2.** Mitochondrial displacement following perturbation with the AFM tip. The AFM tip can be seen as an 'x' shape in the centre of the cell (A, a dotted circle). A region close to the edge of the cell was chosen (A, square), and the trajectories of the mitochondria calculated using ParticleTracker (B, trajectories were emphasized for clarification).

### Nanomechanical force induces significant mitochondrial rearrangements

The results reveal that ~80% of cells displayed an increase in mitochondrial displacement over the basal movements within each cell, whereas ~20% of the cells displayed an interesting decrease in displacement. This behaviour could reflect the dynamic relationship of mitochondria with the cytoskeleton, for example naturally or mechanically induced dissociation of the mitochondria from the cytoskeleton. Extending the analysis to the total number of mitochondria analyzed ( $n=323$ ), we found that the average basal

displacement of mitochondria was  $114 \pm 6$  nm. After pushing with the AFM tip, the displacement increased to  $160 \pm 10$  nm ( $*P < 8E-7$ ) (Figure 3). Therefore, locally applied forces over the nucleus induced a statistically significant rearrangement of mitochondria at the cell edges (~26  $\mu$ m from the point of contact), increasing 39.7% following indentation.

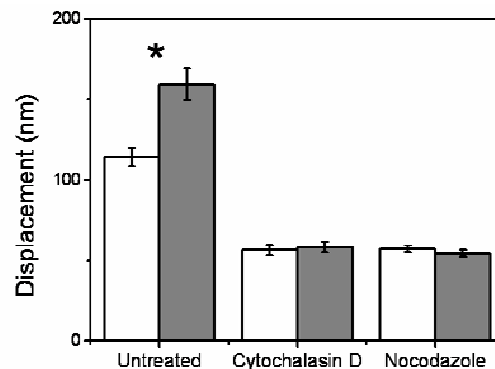


**Figure 3.** Comparison of the difference in mean average displacement of mitochondria between the control (white bars) and the post-perturbation (gray bars) images for untreated cells and for cells treated with the drugs CytD and Nocodazole. The average displacement of the mitochondria analyzed in untreated cells increased in ~40% in response to perturbation with the AFM tip, while in cells treated with CytD or with Nocodazole there was no statistically significant difference between the pre- and post-perturbation displacements.

### Anti-cytoskeletal drug experiments

To investigate the role of the cytoskeleton in transmitting force, we used Cytochalasin D (CytD) and Nocodazole to disrupt the actin and microtubule networks, respectively [18]. Figure 3 shows the average displacement before and after indentation for each set of conditions. The average natural displacement of mitochondria in cells treated with CytD was  $56 \pm 3$  nm and  $58 \pm 3$  nm ( $n=341$ ,  $P > 0.6$ ) after perturbation with the AFM tip. For Nocodazole-treated cells, the average natural displacement was  $57 \pm 2$  nm and  $54 \pm 2$  nm ( $n=320$ ,  $P > 0.3$ ) after perturbation. The results show no statistically significant difference between the pre- and post-perturbation displacements, in both cases. This clearly shows that mitochondrial displacements following a locally applied force are completely dependent on both an intact actin and microtubule cytoskeletal network.

## 4. DISCUSSION AND CONCLUSIONS

In this study we used the feature point tracking algorithm to follow the movement of fluorescently-tagged mitochondria inside living cells. We then calculated the magnitude of displacement following perturbation with the AFM tip, and compared the values to the displacement calculated for natural mitochondrial movement. The results clearly showed that application of nanomechanical forces on cells induce a significant displacement of mitochondria that is far from the point of stress. By chemically degrading the

cytoskeleton it is clear that force-induced mitochondrial displacements are dependent on both the actin network and the microtubules.

The use of the feature point tracking algorithm for tracking displacement of individual mitochondrial structures proved to be fast and accurate. Being independent of specific motion models, this algorithm is highly suitable in this case, where both natural and force-induced motion of mitochondria needs to be analysed. Furthermore, the particulate morphology of the mitochondria, and the usual dispersed arrangement of mitochondria at cell edges, made it easier to track. As the analysis was restricted to only 3 images spread over 3 seconds, false detections and linkage by the automated process were generally avoided. Moreover, all trajectories were manually validated to remove these false detections and to assure the accuracy of the results. Indeed, when there is a need to track mitochondria over longer times, false linking of separate mitochondria on sequential frames can occur, and should be taken into consideration.

## 5. ACKNOWLEDGEMENTS

YS is funded by a CASE studentship from the BBSRC and Unliver. MAH is supported by the Wellcome Trust. AEP is funded by a grant from the "Dr. Mortimer and Mrs. Theresa Sackler Trust".

## 6. REFERENCES

- [1] G. Binnig, C. F. Quate, and C. Gerber, "Atomic Force Microscope," *Physical Review Letters*, vol. 56, pp. 930-933, 1986.
- [2] C. A. Putman, K. O. van der Werf, B. G. de Grooth, N. F. van Hulst, and J. Greve, "Viscoelasticity of living cells allows high resolution imaging by tapping mode atomic force microscopy," *Biophys. J.*, vol. 67, pp. 1749-1753, 1994.
- [3] M. Radmacher, R. W. Tillmann, M. Fritz, and H. E. Gaub, "From Molecules to Cells - Imaging Soft Samples with the Atomic Force Microscope," *Science*, vol. 257, pp. 1900-1905, 1992.
- [4] G. Charras and M. A. Horton, "Cellular mechanotransduction and its modulation: An Atomic Force Microscopy study," *Biophysical Journal*, vol. 80, pp. 305A-306A, 2001.
- [5] C. Rotsch, K. Jacobson, and M. Radmacher, "Dimensional and mechanical dynamics of active and stable edges in motile fibroblasts investigated by using atomic force microscopy," *PNAS*, vol. 96, pp. 921-926, 1999.
- [6] A. E. Pelling, S. Sehati, E. B. Gralla, J. S. Valentine, and J. K. Gimzewski, "Local Nanomechanical Motion of the Cell Wall of *Saccharomyces cerevisiae*," *Science*, vol. 305, pp. 1147-1150, 2004.
- [7] B. J. Haupt, A. E. Pelling, and M. A. Horton, "Integrated Confocal and Scanning Probe Microscopy for Biomedical Research," *TheScientificWorld Journal*, vol. 6, pp. 1609-1618, 2006.
- [8] I. F. Sbalzarini and P. Koumoutsakos, "Feature point tracking and trajectory analysis for video imaging in cell biology," *Journal of Structural Biology*, vol. 151, pp. 182-195, 2005.
- [9] J. A. Helmuth, C. J. Burckhardt, P. Koumoutsakos, U. F. Greber, and I. F. Sbalzarini, "A novel supervised trajectory segmentation algorithm identifies distinct types of human adenovirus motion in host cells," *Journal of Structural Biology*, vol. 159, pp. 347-358, 2007.
- [10] H. Ewers, A. E. Smith, I. F. Sbalzarini, H. Lilie, P. Koumoutsakos, and A. Helenius, "Single-particle tracking of murine polyoma virus-like particles on live cells and artificial membranes," *Proceedings of the National Academy of Sciences of the United States of America*, vol. 102, pp. 15110-15115, 2005.
- [11] M. F. Langhorst, G. P. Solis, S. Hannbeck, H. Plattner, and C. A. O. Stuermer, "Linking membrane microdomains to the cytoskeleton: Regulation of the lateral mobility of reggie-1/flotillin-2 by interaction with actin," *Febs Letters*, vol. 581, pp. 4697-4703, 2007.
- [12] C. Brunner, C. Wahnes, and V. Vogel, "Cargo pick-up from engineered loading stations by kinesin driven molecular shuttles," *Lab on a Chip*, vol. 7, pp. 1263-1271, 2007.
- [13] A. P. Manderson, J. G. Kay, L. A. Hammond, D. L. Brown, and J. L. Stow, "Subcompartments of the macrophage recycling endosome direct the differential secretion of IL-6 and TNF alpha," *Journal of Cell Biology*, vol. 178, pp. 57-69, 2007.
- [14] B. G. Sengers, M. Taylor, C. P. Please, and R. O. C. Oreffo, "Computational modelling of cell spreading and tissue regeneration in porous scaffolds," *Biomaterials*, vol. 28, pp. 1926-1940, 2007.
- [15] Y. R. Silberberg, A. E. Pelling, W. R. Crum, D. J. Hawkes, and M. A. Horton, "Mitochondrial Displacements in Response to Nanomechanical Forces," *J. Molecular Recognit.*, pp. in press, 2007.
- [16] R. Levy and M. Maaloum, "Measuring the spring constant of atomic force microscope cantilevers: thermal fluctuations and other methods," *Nanotechnology*, vol. 13, pp. 33-37, 2002.
- [17] A. E. Pelling, D. W. Dawson, D. M. Carreon, J. J. Christiansen, R. R. Shen, M. A. Teitell, and J. K. Gimzewski, "Distinct contributions of microtubule subtypes to cell membrane shape and stability," *Nanomedicine*, vol. 3, pp. 43-52, 2007.
- [18] G. T. Charras and M. A. Horton, "Determination of Cellular Strains by Combined Atomic Force Microscopy and Finite Element Modeling," *Biophys. J.*, vol. 83, pp. 858-879, 2002.